Waste Biomass Valor (2016) 7:9–21
DOI 10.1007/s12649-015-9431-y

ORIGINAL PAPER

Thermomechanical Characterization of Waste Based TESM and Assessment of Their Resistance to Thermal Cycling up to 1000 °C

Antoine Meffre[1,4] · Nicolas Tessier-Doyen[2] · Xavier Py[1] · Marc Huger[3] · Nicolas Calvet[1,5]

Received: 13 May 2015 / Accepted: 1 September 2015 / Published online: 8 September 2015

Abstract The aim of this work has consisted to study the ability of an innovative thermal energy storage material called Cofalit to withstand thermal shocks under repeated thermal cycles up to 1000 °C. Starting thermomechanical properties (Young's modulus and thermal expansion coefficient) have also been characterized from room temperature to 1000 °C respectively by non destructive pulse-echography technique and standard dilatometric equipment. As these parameters are strongly dependent on the microstructure evolutions of such Cofalit materials when the temperature evolves, complementary scanning electron microscopy observations have been performed. With a concentrating solar test facility, severe thermal cycles have been imposed at the surface of the tested materials between 500 and 1000 °C. Critical shock and ageing experimental results up to 2500 °C emphasize the sufficient refractoriness. This study highlights the wide potential of this Cofalit material for high temperature applications.

Keywords Concentrated solar power (CSP) · Solar energy · Thermal energy storage (TES) · Recycled waste · Refractory ceramic · Microstructure · Life time · High temperatures · Thermomechanical properties

Abbreviations

ACW	Asbestos containing waste
CAES	Compressed air energy system
EDS	Energy dispersive spectrometry
XRD	X-ray diffraction
SEM	Scanning electron microscopy
TES	Thermal energy storage
TESM	Thermal energy storage material
STESM	Sustainable thermal energy storage material
GHG	Green house gas
E	Young's modulus (GPa)
CTE	Coefficient of thermal expansion ($\times 10^{-6}$ K^{-1})

Introduction

The development of concentrated solar power plant technologies is limited by the following major drawbacks: (1) the shift between the solar source availability and the industrial or domestic demands, (2) the solar source variation during daytime or over seasons and (3) the dynamic solar intermittencies (day/night and clouds). To answer those constraints, the two conventional solutions are the hybridization (the solar field is partly or totally replaced by another thermal source as fossil energy when needed) and the storage of thermal energy (mainly TES systems based on sensible heat [1]).

✉ Xavier Py
py@univ-perp.fr

1 PROMES CNRS UPR-8521, University of Perpignan Via Domitia, Rambla de la Thermodynamique Tecnosud, 66100 Perpignan, France

2 Groupe d'Etude des Matériaux Hétérogènes (GEMH), Centre Européen de la Céramique (CEC), 12 rue Atlantis, 87068 Limoges Cedex, France

3 Laboratoire de Science des Procédés Céramiques et Traitement de Surface (SPCTS), UMR CNRS 6638, Centre Européen de la Céramique (CEC), 12 Rue Atlantis, 87068 Limoges Cedex, France

4 Eco-Tech-Ceram co., INSOL - Site Carnot, Rambla de la Thermodynamique Tecnosud, 66100 Perpignan, France

5 Present Address: Masdar Institute of Science and Technology, PO Box 54224, Abu Dhabi, United Arab Emirates

Considering that the hybridization using a fossil source reduces the renewable character of the technology, TES presents today an increasing interest. The storage technology currently acknowledged industrially today is the two tanks molten solar salt. Nitrates mixtures ($NaNO_3$/KNO_3, or other ternary mixtures) are used in the molten state simultaneously as heat transfer fluid and/or storage material. For industrial applications, such as the Andasol 1 concentrated solar power (CSP) plant in Granada (Spain), 28,000 tons of solar salts materials are required to store 1125 MWh for 7.5 h of capacity [2]. Taking into account the acknowledgements of the global warming, the international experts have estimated that about 630 GWe of CSP should be built in 2050 in order to reach the energy security targets. Considering that about 700 MWe are already built today, roughly, 400 more Andasol like plants of 50MWe would be needed every year corresponding to the consumption of 9–20 times the world production of nitrates from mines. This thermal storage technology developed during the eighties is not adapted to the current environmental or economical constraints [3]. Beside those mature CSP plants, expected future ones should be operated at higher temperature ranges (up to 800 °C) using air as heat transfer fluid. In this case those salts are not concerning any more. Hot air is used as working fluid in central receiver CSP systems based on the Solar Gas Turbine (SGT) technology first studied through research project like SOLGATE and demonstrated at pilot scale in the SOLUGAS plant in Spain. As noticed in the corresponding literature [4], these so-called SGT CSP technologies are operated below 1000 °C. Hot air is also considered as alternative HTF for parabolic trough CSP system for which the maximum expected temperature level is 650 °C [5].

In both ACAES and CSP, the TES sub system is operated under the so-called direct passive regenerator configuration [6, 7]. This means that the heat transfer fluid employed in the process is directly used as heat transfer fluid in the TES system, in direct contact with the storage media. Therefore, a ceramic material is placed in the envelop of the TES in the form of structured packing of stacked flat or corrugated plates between which the heat transfer fluid, hot air, is flown. During the charging step, hot air from the CAES compressor or from the solar receiver is fed to the entrance of the TES unit initially at the low temperature level. Under discharge, cold air from the ACAES cavern is flown through the TES unit under reverse direction to be heated before the turbine. In the case of CSP, heat from TES is used when the power or temperature level at the outlet of the central receiver is not high enough.

Very few materials are suitable for the specific requirements of TES for CSP industrial applications. In sensible heat based thermal energy storages (TES), storage materials are submitted to cyclic variations in temperature during the whole expected life-time of the process. Then those TESM have to withstand hundreds to thousands of thermal cycles, sometimes under pressure and corrosive contact with heat transfer fluids. Under operation, a life time of 30 years is one of the major requirements established in 2008 by the International Energy Agency (IEA) in Bad Tölz [1]. Both a suitable refractoriness and a significant ability to withstand thermal fatigue (repeated thermal shocks) are required for materials devoted to such temperature applications. High performance industrial refractory ceramics elaborated at very high temperature such as electrofusion or sintering (for example fully dense Alumina–Zirconia-Silica products employed for glass manufacturing or Silicon Carbide based low cement castables used in heat regenerators) [8, 9] are the most recommended materials. A wide use is strongly limited by the high cost of these refractory products ranging from 6000 to 8000 €/ton. Elaborated from mixtures of different selected raw materials with controlled heating and cooling during the processing, this kind of material represents an important environmental payback time. As the conventional molten salt technology, such an approach is not really in agreement with sustainable development. In this context, major recent efforts have been recently devoted to find alternative TES materials with high availability, low-cost, good (thermal) fatigue and thermal shock resistance, and exhibiting preferably a favorable sustainable behavior.

In this field, recent candidates based on recycled ceramic materials from vitrified industrial waste, namely Asbestos Containing Waste (ACW), have been already proposed [10]. Fully melted when heated up to 1500 °C by plasma torch technology, the hazardous fiber character of ACW is then completely removed [11]. Up to now without any valuable commercial application, the obtained products are simply poured in a cast iron mold ($1 \times 1 \times 0.5$ m^3) and submitted to a natural cooling during which important thermomechanical stresses can occur. The final crystallized product is often used as road filler materials. Even if the resulting industrial ceramic ingots are usually cracked, those raw ceramics exhibit interesting thermophysical properties such as a high stability up to 1000 °C under air atmosphere and a low commercial price (in the range of 8–10 €/t) compared to corresponding commercial silicate oxides based refractory materials. Comparatively, by controlling both chemical composition and solidification kinetic process (meaning the cooling step), appropriate ceramic microstructures strongly related to efficient thermomechanical properties could be obtained. The initial complex chemical composition of the waste allows the formation of different possible crystallized phases [10] whose chemical nature, morphology, size and amount are

deeply related to the cooling operating conditions. Each phase exhibits its own coefficient of thermal expansion which can induce micro defects such as inter and intragranular micro-cracks. Recent works [12, 13] have shown that a moderate micro-cracked microstructure can significantly improve the whole thermal shock resistance of such refractory materials: the non-linear mechanical behavior induced by diffused micro-cracks allows a higher strain to rupture. As a consequence, the occurrence of a probable catastrophic failure of parts, when submitted to repeated thermal cycles, is limited. In the proposed approach, a recycled ceramic material can be used in the regenerator configuration widely employed in the metallurgic or glass industries. In the case of CSP applications, theoretical studies or pilot experiments [14, 15], consider such solid media in the form of granular bed, bricks or shaped monoliths. The solid media is considered as non porous and channels formed by the porosity of the packed bed itself or intentionally included in the bricks are offered to flow the HTF. This approach allows specific optimizations based on the definition of the solid wall thickness and air channel diameter leading to proper TESM efficiency, best heat transfer coefficients for lowest pressure drops. Pressure drop studies have to be performed for each specific configuration (packing geometry) and operating parameters (temperature levels, mass flow, pressure level). During its whole life time, the sustainable thermal energy storage material is expected to ensure a good thermomechanical resistance with regard to thermal cycles. This specific critical property has to be assessed.

In this study, thermomechanical properties of two Cofalit samples exhibiting different chemical compositions have been characterized in temperature from room temperature up to 1000 °C under air atmosphere for two successive thermal cycles. Note that these experimental tests are only focused on initial properties of Cofalit materials: indeed, these values are highly needed for further comparisons after extended thermal cylcing tests. During this heat treatment, the Young's modulus (E) evolution has been measured by pulse echography technique in long bar mode [16]. As E is a high sensitive parameter with respect to microstructural changes, its evolution can offer relevant informations concerning thermal shock resistance and life-time expectancy under operating conditions. Advantageously non destructive and operating in situ, this method is also very well adapted to characterize heterogeneous samples containing coarse aggregates and defects (e.g. porosity, cracks). Those Young's modulus measurements have been also correlated to SEM observations and thermal expansion measurements. This comparison has been carried out to understand the different microstructural mechanisms occurring during the heating/cooling steps in order to identify the operating temperature range in which the ceramic could be used without catastrophic damage.

Finally, Cofalit samples have been tested under repeated thermal cycles using a concentrated solar test facility linked to a temperature controlled loop device. Under concentrated solar flux, only one face of the sample is heated. This equipment allows to monitor a heating rate at the surface up to 2500 °C/min. Comparatively to the above complementary echography and thermal expansion techniques operating at a lower heating rate (5 °C/min), thermal shock severity and aging have been enhanced. During these severe thermal cycles, the temperature profile inside the cylindrical sample has been measured to highlight the stability of the material.

Refractory Materials Processing and Experimental Procedure of Characterization

Studied Materials

The studied refractory ceramic (Cofalit) is produced by the INERTAM-EUROPLASMA company in France from ACW. In the current industrial process, ACW mixtures are molten up to 1500 °C (1) to remove the Asbestos hazardous character due to its fibrous morphology and (2) to ensure the sufficiently low viscosity required to cast the inert product inside an iron ingot mold. During the cooling process, the thermal flux is decreasing from the skin to the center of the ingot due to the increasing thermal resistance. This induces a complex but already well known microstructure [17, 18] composed of a covering peripheral glassy layer followed by a thin layer of small and randomly distributed equiaxed crystals. Deeper in the block, where the temperature gradient has been well established, the crystals have preferentially grown in the same direction and constitute an organized assembly similar to columnar crystallites. More deeper, the crystals in the core of the ingot have grown a little more with different kinetics of growth depending on the direction leading to various shapes depending on (1) their individual chemical composition, (2) the maximum working temperature and (3) the cooling rate. The very severe temperature gradient between the skin and the center of the part involves some macroscopic brittle failures induced by critical cracks. Until now, the industrial efforts have been successfully focused on (1) the removing of hazardous fiber character and (2) the reduction of the cost, regardless to the thermomechanical performances of final materials.

Among the various structural types of Cofalit materials described above, two samples have been selected (COF I and COF II) in the second structural zone of an industrial ingot volume containing small and randomly distributed

equiaxed crystals. Consequently, the two selected samples for this study are raw industrial materials manufactured without any specific cooling protocol. The type of microstructure has been selected as being the most promising for suitable mechanical properties [19, 20]. Oxide compositions of both samples have been determined by energy dispersive X-ray spectrometry (EDS) and are presented in Table 1.

The composition of the two industrial samples (COF I and COF II) belonging to silicate based refractory group is mainly composed of three major oxides ($\approx$80 wt%) in the ternary system SiO_2, Al_2O_3 and CaO. Wollastonite ($CaSiO_3$) and Augite ($CaMgSi_2O_6$) are the main identified crystallized phases [21]. The so-called "average" chemical composition corresponds to an average calculation taking into account chemical oxide proportions data measured by the INERTAM Company taking into account a large number of Cofalit samples during 10 years [22]. Even if the SiO_2/CaO ratio is slightly higher for COF I and COF II, these two compositions are not so different from the average one. This implies that the results obtained in this study can be rather fairly generalized to all Cofalit materials. The last column of Table 1 indicates the total wt% of minor other oxides as impurities representing about one third of the periodic table elements. Acting as nucleating agents, some of these impurities can induce germination whereas others may decrease the crystallization temperature such as ferric (Fe^{3+}) cations [23]. The higher the ionic field force is, the smaller is the temperature of devitrification and the thermal stability of the material. As the chemical proportion of ferric oxide contained in COF I and COF II compositions is significantly different (equal to 5.2 and 12.8 wt% respectively), it is assumed to have an influence on the thermomechanical behavior.

Experimental Procedure of Characterization

SEM Observations of the Microstructure

The microstructure of samples has been observed by scanning electron microscopy [StereoScan 260, Cambridge Instruments]. After polishing (3 μm), sections have been chemically etched (deposition of a 10 % diluted hydrofluoric acid drop during 10 s) to slightly dissolve the remaining amorphous phases at the surface. Contrast between the different phases of the material is then favored during SEM observations. The SEM observations have been performed before and after thermal expansion and elastic properties characterization heat treatments for comparison.

Thermal Expansion Behavior

Measurements have been carried out using a commercial dilatometer Netzsch DIL 402 PC, with squared cross section samples of $5 \times 5 \times 20$ mm^3 in external dimensions. The slope of the curve $\Delta L/L_0 = f(T)$ is the so-called coefficient of thermal expansion (CTE) calculated within the considered temperature range of interest. The linear thermal expansion has been measured under two successive identical thermal cycles (Fig. 1). Heating and cooling rates have been fixed at a value of 5 °C.min^{-1} with a plateau of 1 h at the maximum temperature (1000 °C).

Pulse Echography Technique

Young's modulus measurements have been carried out using a high temperature ultrasonic technique operating in a "long bar" mode (the lateral dimension of the propagation medium is smaller than the wavelength). This method, whose principle has been already detailed elsewhere [22], has been already been successfully used to investigate the elastic behavior of various ceramics for temperatures up to 1750 °C [24]. Ultrasonic compressional waves are generated by a magnetostrictive transducer and are sent toward the parallelepipedic sample through an alumina wave guide. The transfer at the interface between the guide and the sample is ensured by an aluminous refractory cement (Fig. 2).

Electronic equipment (signal acquisition by a digital oscilloscope and a specific software package) automatically measures and records the time delay τ corresponding to one round-trip of the wave through the sample. Then, the Young's modulus E of the material is calculated with the following equation:

$$E = \rho \times (2L/\tau) \quad (1)$$

where L and ρ are the sample length and apparent density, respectively. The different characteristics of the ultrasonic line components have been adapted to highly heterogeneous refractory concretes exhibiting large grains and/or a high pore volume fraction (a low frequency of 110 kHz

Table 1 Chemical oxide composition of raw Cofalit [10] (in wt%)—*EDS/**ICP

Oxides (wt%)	SiO_2	CaO	Al_2O_3	MgO	Fe_2O_3	K_2O	TiO_2	Others
COF I*	43.6	27.2	10.6	5	5.2	0.2	1	7.2
COF II*	42.5	24.6	8.8	2.9	12.8	0.6	1	6.8
Average**	38.8	32.3	6.7	6.1	6.6	0.6	0.6	8.2

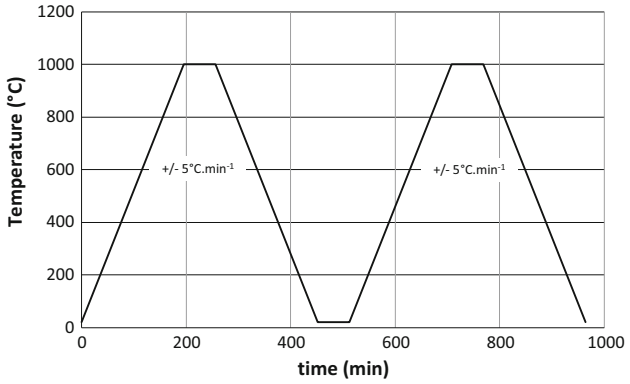

Fig. 1 Thermal cycle used for characterization tests

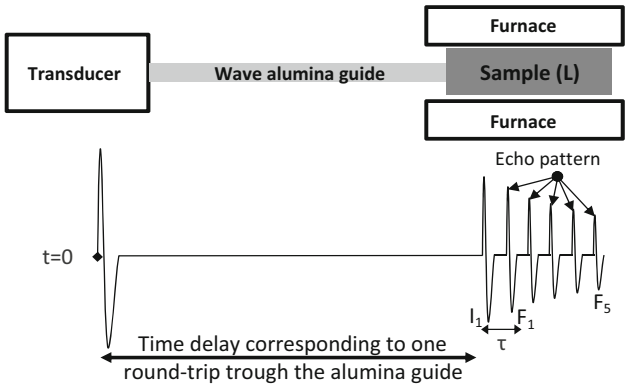

Fig. 2 Schematic representation of the pulse echography apparatus

and typical dimensions of 11 × 11 × 120 mm^3 for these studied Cofalit specimens). Ultrasonic and thermal expansion measurements have been performed under the same operating conditions (Fig. 1): a rate of 5 °C/min for heating and cooling steps and a 1 h isothermal plateau at 1000 °C.

High Temperature Dynamic Fatigue Tests Under Concentrated Solar Flux

Under operation, thermal energy storage materials are currently subjected to severe interfacial thermal flux and strong and repeated internal temperature gradients. In the case of future gas turbine CSP tower generation, the needed sustainable thermal energy storage materials should be designed to operate between 500 and 1000 °C under hot air as heat transfer fluid. Dynamic solar intermittencies (induced by cloud effects) could induce very significant thermal shocks (in temperature and power), toward the TES unit. Therefore, it is first necessary to verify the stability of their properties and their resistance to thermal cycling. In other words, relevant assessments are needed to check the ability of the material structure to sustain thermal fatigue induced by repeated thermal cycling and to thermal shocks.

According to heat flux in concern, such assessment could not be properly achieved using conventional electric oven. Then, particular experimental conditions have been performed at the solar furnace of Odeillo using a specific original device based on a vertical axis parabola of 2 m in diameter illustrated in Fig. 3. Within the temperature range of industrial applications (500–1000 °C), a sample in the form of a cylinder (200 mm in length and 25 mm in diameter) has been submitted to different thermal cycles under atmospheric air, the solar beam being focused on the surface. In order to obtain an axial thermal gradient through the cylinder, only its upper surface was irradiated by the concentrated solar flux while all its peripheral surface was insulated with a 60 mm thick rock-wool layer covered by an external rigid metallic casing. The module was placed on a trolley allowing to easily submit the upper surface of the sample to the parabola focused beam or to withdraw it when cooled. Under advantageous sunny conditions, a heliostat mirror is used to reflect the sun light to the vertical axis parabola trough a set of carbon blades. A temperature controller is used to drive the opening of the carbon made blades fast shutter with respect to the surface temperature of the lighted material measured by a solar-blind pyrometer located above the sample (at the center of the parabolic mirror). The controller regulates the surface temperature of the sample in agreement to predetermined temperature patterns, even compensating the variations of the incoming solar energy due to changing weather conditions. Three K thermocouples have been placed respectively at 10, 25 and 40 mm from the irradiated surface to measure the axial temperature profile in the center of the cylinder (Fig. 4). In the present paper, this equipment is used to observe qualitatively the thermal shock effects and the fatigue resistance of the tested materials within the following working conditions: surface flux up to 16 MW/m^2, surface temperature from room temperature up to 1000 °C and heating rate range from 100 to 2500 °C min^{-1}. Furthermore, under stabilized periodic regime, the axial temperature phase lag and shift measured between two successive thermocouples leads to the identification of the thermal diffusivity of the material [25, 26]. This particular aspect, out of the scope of the present study, will be developed in a further publication. The combination of the above US technique, the original concentrated solar fatigue tests equipment and SEM microscopy is used in the present paper to study the ability of the recycled ceramics to bear repeated thermal cycling under controlled thermal amplitudes and heating rates.

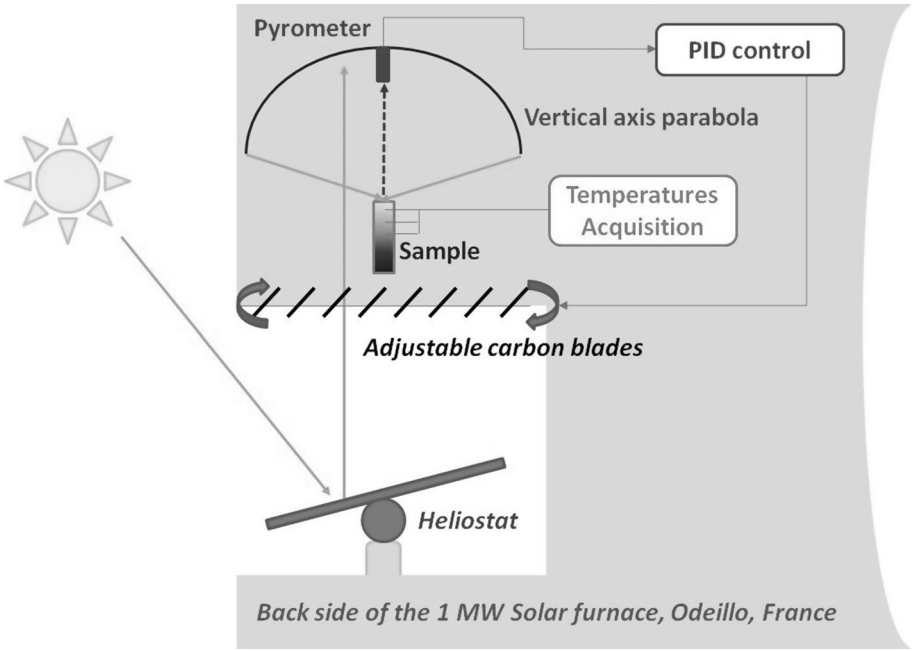

Fig. 3 Representation of the concentrated solar test facility at the PROMES CNRS laboratory in Odeillo France

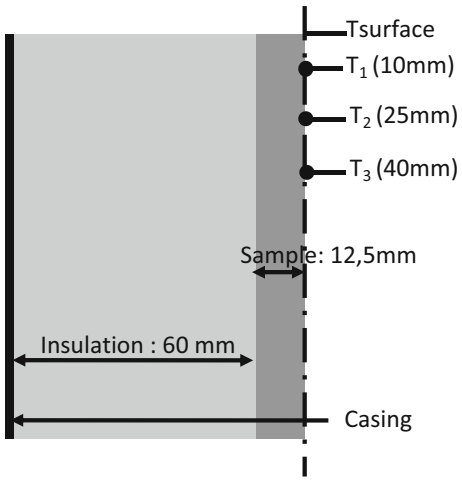

Fig. 4 Positions of the thermocouples in the Cofalit sample during the high temperature dynamic fatigue test under concentrated solar flux

Results and Discussion

Relation Between the Elaboration Process Operating Parameters and the Microstructure

The SEM pictures of Cofalit samples I and II are presented in Fig. 5 at a same magnification level (200 times). The corresponding microstructures have been observed before and after the two successive thermal cycles described above. Comparing the obtained pictures of the two raw samples COF I and COF II (Fig. 5a, b), no main difference can be observed between the microstructures of the two materials. Both of them are composed of randomly distributed dendrite crystals surrounded by a mainly crystallized matrix. The particular shape of crystals observed in Fig. 5 is due to the isotropic thermal flux established in this part of the matter during the solidification step. In a previous work [10], different crystal phases have been already identified by X-Ray Diffraction (XRD). Wollastonite and Augite represent respectively the crystal matrix and dendrite crystals. Even if the obtained material is quasi-fully dense, small isolated closed pores ($\approx$70 µm) can be observed. This microstructure is quite similar to this observed for electrofused zirconia refractories [8, 24]. Metal oxides, principally ferrous oxides, are much more present in COF II sample than in COF I. Therefore during the heating step, the slight decrease observed for COF II thermomechanical properties could be expected at a lower temperature than for COF I.

No significant effect of the thermal treatment (1000 °C, 1 h, air) on both microstructures can be observed (Fig. 5c, d). At the selected scale, before and after the heat treatment, samples remain almost similar. In perfect agreement with DSC and XRD results obtained from a previous study [10, 21], this observation means that crystallized phases in both materials which have been formed during the first industrial cooling step are stable under thermal cycles up to 1000 °C.

According to the literature [12], during the cooling step, two types of cracks can occur due to internal thermal stresses:

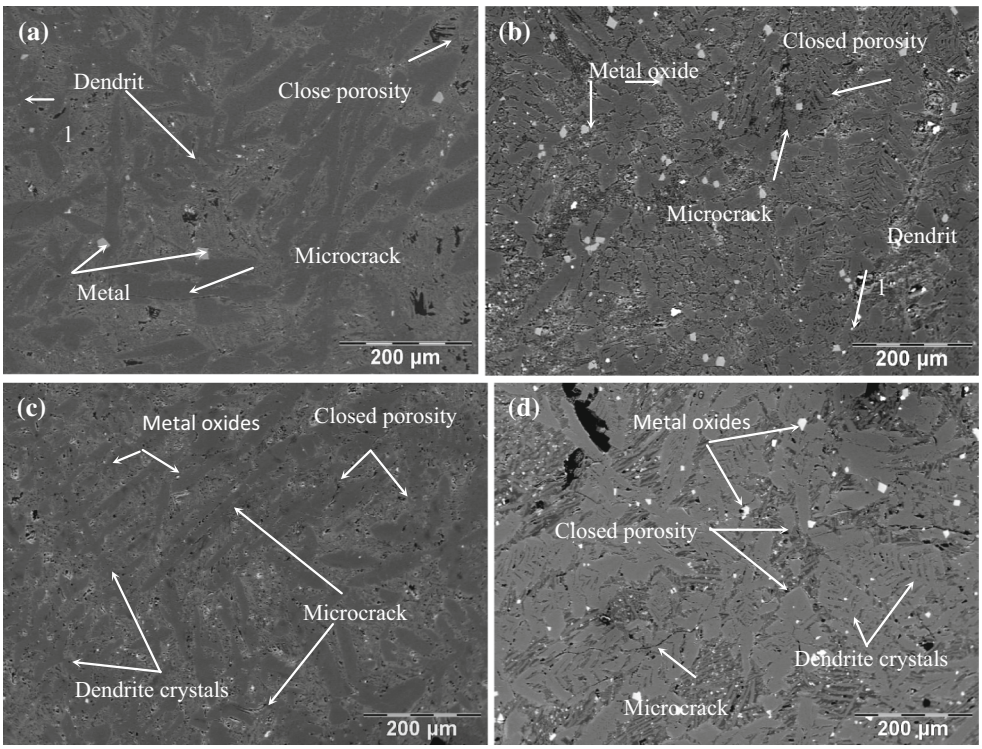

Fig. 5 SEM microcructure of COF I and COF II before and after thermal treatment. **a** COF I before thermal treatment. **b** COF II before thermal treatment. **c** COF I after thermal treatment. **d** COF II after thermal treatment

1. Open macrocracks, easily optically evidenced, due to significant thermal gradients. This type of crack would lead to catastrophic failure of the material part.
2. Diffused micro-cracks (inter or intra grains) induced during the cooling step by the difference in coefficient of thermal expansion between the different crystal phases of the microstructure and the matrix (see Fig. 5c). Rather difficult to observe by SEM microscopy because of their too small thickness, these cracks are not critical for the mechanical behavior of the materials because of their quite energetic stability.

Such micro-structural defects are currently present in heterogeneous materials such as in industrial refractories devoted to steel or glass applications [27].

The detailed observation of those micro-cracks is rather difficult and remains highly qualitative due to two main reasons: (1) the thickness of the micro-cracks induced by the difference in coefficient of thermal expansion between the different crystal phases depends strongly in the temperature level and should be observed locally during the thermal treatment up to 1000 °C to be assessed properly, (2) the whole effect results from the contribution of numerous micro-cracks of different nature (involving different crystal phases and structures) and consequently the observation of few micro-cracks evolutions would be not really representative.

Coefficient of Thermal Expansion (CTE) and Young's Modulus (E) Under Moderate Thermal Cycling

In order to evaluate starting thermomechanical properties of the sample COF I under thermal cycles, CTE (slope of the ΔL/Lo curve) and E curves have been plotted on the same graph (Fig. 6). The curves corresponding to the first thermal cycle are the dash ones whereas curves corresponding to the second thermal cycle are continuous. From a general point of view, E variations present a hysteresis typical from refractory ceramics mainly composed of SiO_2/CaO/Al_2O_3. Comparing the two successive cycles, no significant difference appears in the whole observed behaviors except a slight displacement of the E curve.

According to those measurements and the corresponding literature, the Cofalit ceramic behavior under thermal cycling can be divided in five main domains:

1. Domain A: starting from room temperature up to 300 °C, the E variation in this temperature range is about 10 % and the CTE value remains almost constant.
2. Domain B: from 300 up to 700 °C, Young's modulus increases with temperature ranging from 82 to 105 GPa (+28 %). Within the same domain, the slope of the thermal expansion (CTE) curve behaves in a similar

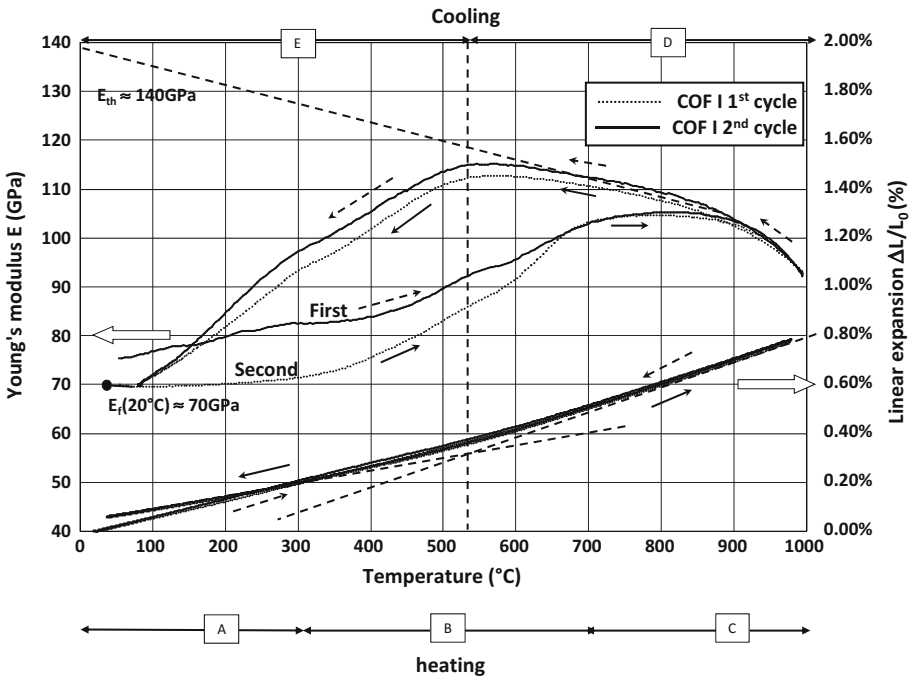

Fig. 6 Young's modulus and linear thermal expansion vs temperature for sample COF I. First cycle *dashed lines*, second cycle *continuous lines*

way, highlighting that the CTE value of the material varies from 6.9 to 9 × 10^{-6} K^{-1}. In fact, interfacial debondings between coarser grains and the matrix, tend to disappear because of a greater mean CTE of crystals [12, 28, 29]. As the initial damage is reduced when the temperature raises, the healing of defects induces an increase of elastic properties, especially near 500 °C, temperature for which a majority of crystallized grains may enter in contact with the matrix.

3. Domain C: under heating from 700 to 900 °C, E reaches a plateau. The highest CTE value obtained at 1000 °C ($CTE_{(1000–900\ °C)} \approx 9 \times 10^{-6}\ K^{-1}$) should result from the cumulative effects of CTE matrix and CTE crystals. In this domain, all debondings between dispersed crystals and the matrix should be closed. At 900 °C, E begins to decrease and at 1000 °C, the value is close to 90 GPa. Beyond a given temperature, phases exhibiting a low viscosity are formed leading to a fall of elastic properties. Ferrous oxide formed at the lowest temperature during the heating step [23] and the few percentage of glassy phase could be responsible for this softening. Additional works are necessary to confirm this assumption. Nevertheless, these phases allow the material to heal over. At the end of this stage, the material is almost fully cured, and can be considered as free of stress.
4. Domain D: Under cooling from 1000 to 550 °C, Young's modulus increases when the temperature decreases. Softest phases solidify, interatomic bondings are rigidified and internal stresses increase in the material but do not reach the strength to rupture value. The E curve follows a linear behavior typical of a free of damage ceramic material [10]. The intercept of the asymptote of this linear behavior with the Y axis leads to an evaluation of the theoretical Young's modulus value of about $E_{th} \approx 140$ GPa. At the end of this D domain, the rigidity of Cofalit is greater than 110 GPa at 530 °C.
5. Domain E: under cooling at the critical value of 530 °C, Young's modulus strongly decreases whith temperature. The internal stresses due to CTE mismatches become sufficiently high to allow the initiation of damage around crystallized grains. The material micro-cracks start to reopen leading to the simultaneous decrease of the Young's modulus and CTE values. This critical temperature of 530 °C corresponds to the quartz transformation (quartz β to quartz α).

At the end of the first thermal cycle, at room temperature, measured E and CTE values are 70 GPa and 6.6 × 10^{-6} K^{-1} respectively. The E value is 7 % below the initial value. This result can be attributed to the elaboration conditions. During the cooling process, the smaller the temperature, the higher the viscosity and consequently the higher the relaxation time to reach the thermodynamic equilibrium. When the viscosity of the mixture reaches the critical value of 10^{12} Pa s, the glass transition temperature is reached and the mobility of atoms is stopped as the thermomechanical stress relaxation occurs. At room temperature, some zones of the microstructure ingot stay under tensile constraints affecting Young's modulus. CTE

doesn't show drastic changes (between 6.6 and 9×10^{-6} K^{-1}) highlighting that no allotropic transformation occurs and that crystallized phases are stable on the whole range of operating temperature.

During the second thermal cycle, between 20 °C up to 1000 °C, thermal expansion is almost linear and quite the same as for the first thermal cycle. The second hysteretic loop observed for E evolution (almost equivalent to the first one) highlights the thermomechanical stability and refractoriness of the Cofalit material in the temperature range (20–1000 °C). According to these results, the raw industrial Cofalit elaborated from wastes and without any controlled cooling step, seems to be very relevant as TESM for the whole kind of CSP and more particularly for future generation of high temperature hot air driven solar thermodynamic power plants working in the operating temperature range above 550 up to 900 °C.

Comparison Between the Two COFALIT Samples

In Fig. 7, Young's modulus and CTE evolutions during the second thermal cycle of the two samples COF I and COF II are compared. Curves corresponding to the first sample are continuous whereas curves corresponding to the second sample are dashed.

The two thermal expansion curves superpose very well below the critical temperature of 530 °C and remain rather similar up to 1000 °C with a maximum difference of 9 % observed at 980 °C. Considering the fact that a CSP industrial thermal energy storage unit would be composed of numerous modules stacked assembled together, a significant variation between their respective CTE would have been prejudicial: mechanical frictions inducing local stresses under repeated thermal cycling would then affect to the overall integrity of the assembly.

Young's modulus of both samples also presents a similar hysteresis loop with the same characteristic temperatures and asymptotic theoretical E_{th} value. E starts to decrease at 900 °C and the reopening of microcracks occurs around 550 °C. Between 900 and 1000 °C, it is interesting to note that the rigidity of COF II sample decreases faster than the COF I one. At 1000 °C, E values are 92 and 80 GPa for sample COF I and COF II respectively. It could be explained by the higher amount of ferrous oxide. Anyway, the observed specific temperatures are very similar. This repeatability of starting properties from a sample to another proves the acceptable efficiency of the current industrial chemical composition control. In order to study the behavior of these materials in more severe conditions, the effect of high velocity thermal cycles under direct concentrated solar radiations under air have been also investigated within the typical temperature range in concern in CSP.

COFALIT Submitted to Severe Operating Conditions

Thermal Shock: Critical and Natural Discharge

As the concentrated solar flux in CSP could be subjected to major and rather unpredictable solar intermittencies, it is necessary to study the thermophysical properties evolution of the TESM occurring during a thermal accident. This approach is experimentally considered through severe cooling tests (quench) using a concentrated solar facility without any mechanical load. A first severe quench

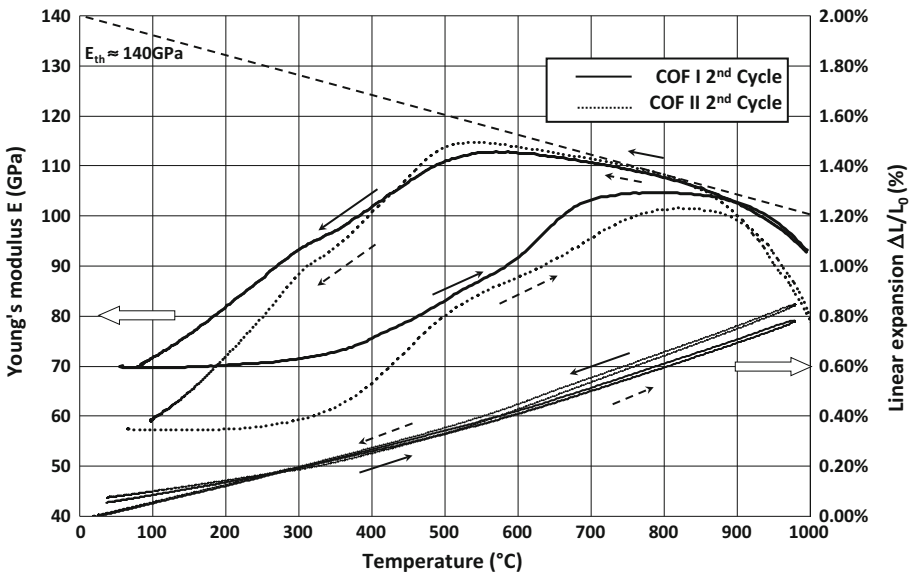

Fig. 7 Young's modulus and linear thermal expansion vs temperature for samples COF I and II during the 2nd heat treatment. COF I 2nd cycle *continuous line* and COF II 2nd cycle *dashed lines*

illustrated in Fig. 8a: after a first thermal loading maintained up to a steady state, a complete thermal discharge from 1000 to 100 °C under flowing compressed air (at room temperature) has been performed to evaluate the mechanical stability of the material during a total intermittency of the heating source.

A second discharge from 1000 to 100 °C under natural convection provides information about the thermal shock resistance during a possible complete stop of heat transfer fluid flow inside a storage unit. On the corresponding curves (Fig. 8), the superficial temperature and temperatures at 10, 25 and 40 mm from the irradiated surface have been followed. The various curves present continuous variations. At the end of these experiments, which have been repeated several times, no critical cracks were observed on tested samples.

After 40 min, the permanent regime under heating is almost reached for the three different thermocouples (750, 500 and 350 °C). At this time, a controlled thermal shock has been imposed: the carbon blades were totally closed and the compressed air was flown on the surface of the sample. The initial decrease of temperature was very sharp. Until 400 °C, the average cooling rates were: −1041, −146 and −38 °C min^{-1} respectively at 0, 10 and 25 mm from the surface. Starting from 750 °C, the temperature at 10 mm decreases very quickly under the critical value of about 500 °C. At the end of the discharge, the sample was still no critically macro-cracked and still conserved a whole integrity.

During the second thermal cycle induced after 60 min, the permanent regime was reached in 40 min. Values indicated by thermocouples 2 and 3 were 500 °C and 350 °C as previously observed. But with thermocouple 1, a value of temperature only equal to 720 °C has been registered. Under constant experimental conditions with respect to the first cycle, this lower temperature highlights a higher thermal resistance in the 10 mm part close to the surface. Additional irreversible microcracks could have been opened due to the high thermal shock occurring during the discharge under compressed air flow.

Fatigue Test Under Dynamic Repeated Thermal Cycling

Thermal cycles upon various frequencies have been applied on the same sample. Ranging between 500 and 1000 °C, the surface has been heated at 100, 300 and 2500 °C min^{-1} (maximum available heating rate of the equipment). Comparing Fig. 9a–c, it can be observed that the higher is the heating rate, the higher is the average temperature, but the lower is the amplitude of thermal wave inside the cylinder. This attenuation is due to the rather low Cofalit thermal diffusivity which is in the range of 6.10^{-7} m^2 s^{-1} [10].

Applying the highest heating rate (Fig. 9a), the thermal wave is totally attenuated after one centimeter depth. The temperature is almost constant and no thermal cycles can be really observed. Furthermore if the frequency of the thermal cycle decreases, then the average temperature decreases too. At 100, 300 and 2500 °C min^{-1}, the average temperature values recorded by the thermocouple at 10 mm are respectively 380, 450 and 500 °C.

The raw cylinder of Cofalit was submitted to extended dynamic tests under various and numerous working conditions. After more than 300 thermal cycles under severe conditions, the thermal properties remained constant and no critical crack was observed. Additional works will be done on thinner samples with adapted heating rates to study

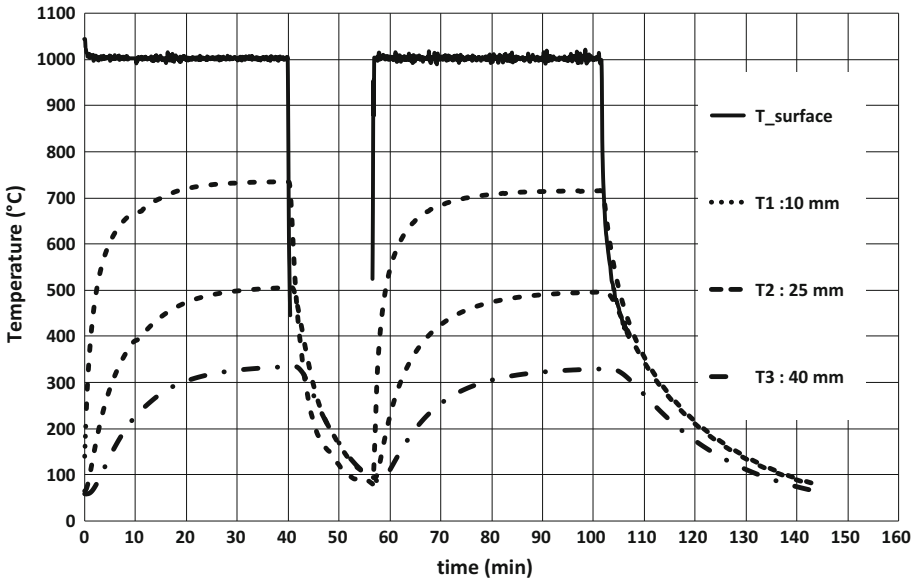

Fig. 8 Local temperature registered by thermocouples in function of the distance from the sample surface during the thermal shock under concentrated solar flux

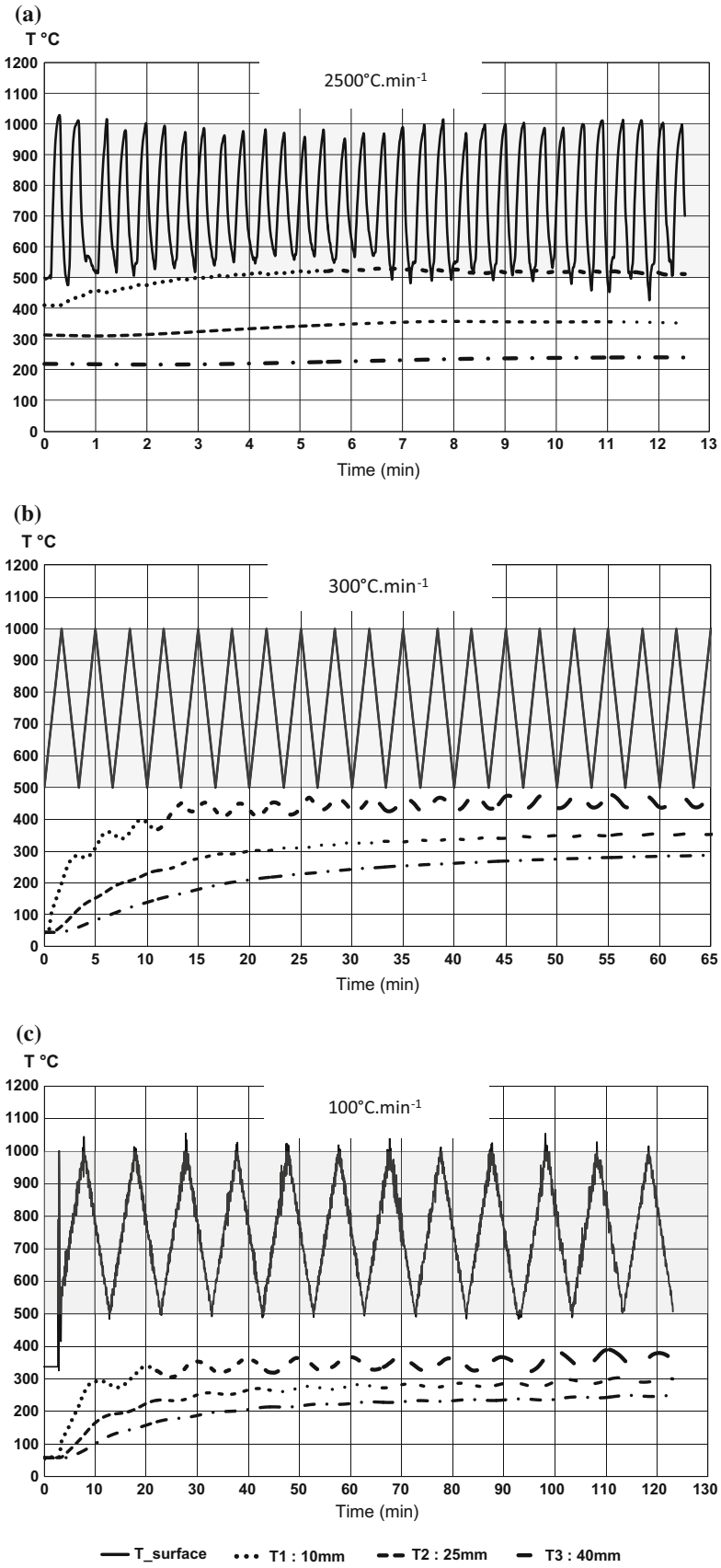

Fig. 9 Thermogrammes in tested material subjected to thermal cycling. **a** Fatigue test under dynamic repeated thermal cycling (2500 °C/min). **b** Fatigue test under dynamic repeated thermal cycling (300 K min^{-1}). **c** Fatigue test under dynamic repeated thermal cycling (100 K min^{-1})

the influence of reopening cracks temperature previously defined by ultrasound investigations.

Conclusion

The Cofalit material which is a recycled ceramic composed of inertised Asbestos Containing Wastes exhibits a repeatable refractory behavior typical from SiO_2–CaO–Al_2O_3 ternary systems. Microstructure of Cofalit is here composed of randomly distributed dendrite crystals surrounded by a crystallized matrix. The mismatch of CTE explained the presence of diffused microcracks which confers to the microstructure the stability and the thermomechanical reversibility during repeated thermal cycles. The repeatability of starting properties after two thermal cycles proves the acceptable efficiency of the current industrial chemical composition control. Therefore, the main future efforts have to be focused on the control of the solidification kinetic in order to avoid large macroscopic critical cracking which can occur during the cooling stage of the processing.

According to Young's modulus and thermal expansion measurements under thermal cycling, Cofalit is proved to be very relevant as TESM for the future solar thermodynamic working temperature range (550–900 °C). After more than 300 severe thermal cycles imposed to a Cofalit cylindrical shaped specimen, no critical cracks have been observed. Additional works are obviously necessary to prove the 30 years expected life time of this refractory ceramic. Coupling pulse echography technique and concentrated solar test facility constitute an efficient way to characterize future TESM under industrial thermal stresses. In situ and non destructive, these methods provide complementary informations about thermal fatigue resistance. Furthermore, by measuring the temperature profiles inside the sample, dynamic experiments offer simultaneously, the possibility to identify the thermal diffusivity according to the periodic permanent regime measurement.

Acknowledgments The project has been supported by the Grant of the French government through the funding of the ANR Stock-E research program SESCO. A very special acknowledgement is dedicated to the French company Europlasma/Inertam for the supplying of numerous samples of ceramics made by vitrification of asbestos containing wastes. The authors also acknowledge the contributions of Mr G. Dejean for the measurement of mechanical properties and to M. Guillot for the design of the temperature control loop.

References

1. IEA: key_world_energy_stats.pdf (2011)
2. Herrmann, U., Kelly, B., Price, H.: Two-tank molten salt storage for parabolic trough solar power plant. Energy **29**(5), 883–893 (2004)
3. Fiorucci, L.C., Goldstein, S.L.: Manufacture, distribution and handling of nitrate salts for solar thermal application. Olin Corporation Report SAND81-8186 UC-62d (1982)
4. Klein, P., Roos, T.H., Sheer, T.J.: Experimental investigation into a packed bed thermal storage solution for solar gas turbine systems. SolarPaces 2013. Energy Proc. **49**, 840–849 (2014)
5. Good, P., Zanganeh, G., Ambrosetti, G., Barbato, M.C., Pedretti, A., Steinfeld, A.: Towards a commercial parabolic trough CSP system using air as heat transfer fluid. SolarPaces 2013. Energy Proc. **49**, 381–385 (2014)
6. Gil, A., Medrano, M., Martorell, I., Lazaro, A., Dolado, P., Zalba, B., et al.: State of the art on high temperature for power generation. Part 1—concepts, materials and modellization. Renew. Sustain. Energy Rev. **14**, 31–55 (2010)
7. Medrano, M., Gil, A., Martorell, I., Potau, X., Cabeza, L.: State of the art on high-temperature thermal energy storage for power generation. Part 2—case studies. Renew. Sustain. Energy Rev. **14**, 56–72 (2010)
8. Patapy, C., Gault, C., Huger, M., Chotard, T.: Acoustic characterization and microstructure of high zirconia electrofused refractories. J. Eur. Ceram. Soc. **29**(16), 3355–3362 (2009)
9. Gallet-Doncieux, A., Bahloul, O., Gault, C., Huger, M., Chotard, T.: Investigations of SiC aggregates oxidation: Influence on SiC castables refractories life time at high temperature. J. Eur. Ceram. Soc. **32**(4), 737–743 (2012)
10. Py, X., Calvet, N., Olives, R., Meffre, A., Echegut, P., Bessada, C., Veron, E., Ory, S.: Recycled material for sensible heat based thermal energy storage to be used in concentrated solar thermal power plants. J. Sol. Energy Eng. **133**, 1–8 (2011)
11. Gomez, E., Rani, D.A., Cheeseman, C.R., Deegan, D., Wise, M., Boccaccini, A.R.: Thermal plasma technology for the treatment of wastes: A critical review. J. Hazard. Mater. **161**(2), 614–626 (2009)
12. Tessier-Doyen, N., Glandus, J.C., Huger, M.: Untypical Young's modulus evolution of model refractories at high temperature. J. Eur. Ceram. Soc. **26**(3), 289–295 (2006)
13. Huger, M., Tessier-Doyen, N., Chotard, T., Gault, C.: Microstructure effects associated to CTE mismatch for enhancing the thermal shock resistance of refractories: investigation by high temperature ultrasounds. Ceram Forum Int. (CFI) **84**(9), 93–102 (2007)
14. Fricker, H.W.: Regenerative thermal storage in atmospheric air system solar power plants. Energy **29**, 871–881 (2004)
15. Zunft, S., Hänel, S., Krüger, M., Dreißigacker, V., Göhring, F.: Wahl. E.: Jülich solar power tower—experimental evaluation of the storage subsystem and performance calculation. J. Sol. Energy Eng. (2011). doi:10.1115/1.4004358
16. Cutard, T., Fargeot, D., Gault, C., Huger, M.: Time delay and phase shift measurements for ultrasonic pulses using autocorrelation methods. J. Appl. Phys. **75**(4), 1909–1913 (1994)
17. Meffre, A., Py, X., Olives, R., Calvet, N., Faure, R., Tessier-Doyen, N., Huger, M.: High temperature TESM thermomechanical characterization and assessment of their resistance to thermal shock. International Innostock, Lleida, Spain (2012)
18. Meffre, A., Py, X., Olives, R., Bessada, C., Echegut, P., Michon, U.: Design and industrial elaboration of thermal energy storage units made of recycled vitrified industrial wastes. In: International ASME Conference, November 2011, Denver Colorado (2011)
19. Joliff, Y., Absi, J., Glandus, J.C., Huger, M., Tessier-Doyen, N.: Experimental and numerical study of the thermomechanical behaviour of refractory model materials. J. Eur. Ceram. Soc. **27**(2), 1513–1520 (2007)
20. Centre d'Animation Régional En Matériaux Avances (CARMA): Les Céramiques Industrielles Applications industrielles et développements potentiels dans les Alpes-Maritimes (1999)
21. Faik, A., Guillot, S., Lambert, J., Véron, E., Ory, S., Bessada, C., Echegut, P., Py, X.: Thermal storage material from inertized

wastes: evolution of structural and radiative properties with temperature. Sol. Energy **86**, 139–146 (2011)
22. INERTAM: Fiche technique du Cofalit. http://www.inertam.com
23. Murat, M., Bachiorrini, A., Negro, A.: Essai de caractérisation des matériaux vitreux à partir des données relatives au phénomène de dévitrification thermique. Revue Phys. Appl. **12**(5), 653–666 (1977)
24. Patapy, C., Gault, C., Huger, M., Chotard, T.: Acoustic characterization and microstructure of high zirconia electrofused refractories. J. Eur. Ceram. Soc. **29**(16), 3355–3362 (2009)
25. Nunes dos Santos, W., Nicolau dos Santos, J., Mummery, P., Wallwork, A.: Thermal diffusivity of polymers by modified angström method. Polym. Test. **29**(1), 107–112 (2010)
26. Fourcher, B., Mansouri, K.: An approximate analytical solution to the Graetz problem with periodic inlet temperature. Int. J. Heat Fluid Flow **18**(2), 229–235 (1997)
27. Massard, L.: Etude du fluage de réfractaires électrofondus du système alumine-zircone-silice. PhD Thesis, École Nationale Supérieure des Mines de Paris (2005)
28. Yeugo Fogaing, E.: Caractérisation à haute temperature des propriétés d'élasticité de réfractaires électrofondus et de bétons réfractaires. PhD Thesis, Université de Limoges, (2006)
29. Petroni, L.: Étude du comportement post-coulée de réfractaires électrofondus à Très Haute Teneur en Zircone (THTZ). PhD Thesis, École Nationale Supérieure des Mines de Paris (2011)